11

Gelation of Magnetic Nanoparticles

Eldin Wee Chuan Lim
National University of Singapore
Singapore

1. Introduction

The study of magnetic nanoparticles and ferrofluids has gained considerable interests among research workers in recent years. The potential range of application that these novel magnetic nanomaterials can offer is gradually being recognized and continues to be explored. As described in a recent review article (Pamme, 2006), magnetic particles have already been used for such diverse applications as the fabrication of ferrofluidic pumps, solid supports for bioassays, fast DNA hybridization, giant magnetoresistive sensors and superconducting quantum interference devices (SQUID). At a more fundamental level, one of the most important and widely investigated aspects of magnetic nanoparticles and ferrofluids is the formation of self-organized microstructures under the influence of an externally applied magnetic field. A suspension of magnetic nanoparticles in a fluid medium can generally be considered as a single magnetic domain with macroscopic properties that are dependent on the properties of individual nanoparticles as well as the interactions between them (Rosensweig, 1985). In the presence of an external magnetic field, the magnetic domain will be oriented in the direction of the field and may approach saturation magnetization. When the external magnetic field is removed, the domain will revert to a randomly oriented state which exhibits no macroscale magnetism. Although it is well-established that the magnetization of a magnetic fluid or ferrofluid is related to the arrangement of the suspended magnetic nanoparticles, which in turn arises due to the effects of interactions between various types of forces present such as Brownian and dipole-dipole interactions for example, current understanding of the kinetics, dynamics and resulting microstructure of the nanoparticle aggregation process is far from complete.

In the research literature, a variety of experimental, theoretical and computational approaches have been applied towards studies of the aggregation and microstructure formation process of magnetic nanoparticles and ferrofluids. In particular, the computational techniques that have been used for such investigations include Monte Carlo simulations (Davis et al., 1999; Richardi et al., 2008), Brownian dynamics (Meriguet et al., 2004, 2005; Yamada and Enomoto, 2008), lattice-Boltzmann method (Xuan et al., 2005), molecular dynamics simulations (Huang et al., 2005), combination of analytical density functional theory and molecular dynamics (Kantorovich et al., 2008), stochastic dynamics (Duncan and Camp, 2006) and analytical methods (Furlani, 2006; Furlani and Ng, 2008; Nandy et al., 2008). Further, several recent studies have also reported comparisons between experimental and theoretical or computational results. For example, the chain formation process of magnetic particles in an external magnetic field and under

the effects of shear in microchannels was analyzed and the chain growth rate predicted by the Smoluchowski model was observed to be consistent with experimental observations (Brunet et al., 2005). The transport of an isolated magnetic microsphere or of very dilute suspensions where dipole-dipole interactions are negligible through a microchannel have also been investigated both experimentally and numerically (Sinha et al., 2007). The controlled aggregation of Janus magnetic nanoparticles was studied using dynamic light scattering and cryo-TEM imaging techniques and the main features of the aggregation behavior were consistent with predictions provided by a modified version of the classic Monte Carlo simulation algorithm (Lattuada and Hatton, 2007). Brownian dynamics has also been applied towards the study of motion of magnetic particles in a magnetic field gradient and shown to be in agreement with experimental measurements based on an optical detection method (Schaller et al., 2008).

While most of the investigations of magnetic nanoparticles dispersions have targeted colloidally stable systems, a few studies have also focused on suspensions undergoing aggregation. Colloidal systems undergoing aggregation exhibit complex behaviors due to several factors such as particle-particle interactions, fractal structure of individual clusters and the aggregation mechanism and kinetics. Several modeling approaches have been proposed in the literature to simulate the aggregation kinetics of colloidal systems, either based on Monte-Carlo simulations, or on population balance equations, or on a combination of the cluster mass distribution computed based on the population balance equations with the structure properties of individual clusters determined by Monte-Carlo simulations (Lattuada et al., 2004a). It was found that the average sizes and structure properties predicted in both the diffusion-limited and reaction-limited aggregation regimes were in good agreement with light scattering measurements (Lattuada et al., 2004b). In the case of magnetic nanoparticles aggregation, both experimental and computational studies have underlined substantial differences between diffusion limited aggregation in the absence and in the presence of an applied magnetic field (Tsouris and Scott, 1995; Promislow et al., 1995; Miyazima et al., 1987). In the presence of magnetic fields, clusters grow as chains aligned in the direction of the applied magnetic field. The kinetics of chain growth has been modeled using Monte-Carlo methods (Miyazima et al., 1987), Brownian Dynamics simulations (Dominguez-Garcia et al., 2007), and population balance equations (Martinez-Pedrero et al., 2008). All of these studies have demonstrated how the average size of chains grows as a power law of time, with an exponent that depends upon the particle volume fraction and the strength of the dipolar interactions (Climent et al., 2004). However, no studies to the best of our knowledge have focused on gelation and percolation of magnetic dispersions at high particles volume fractions.

In this work, we report the first application of a modified version of the Discrete Element Method (DEM) towards the simulation of magnetic nanoparticle aggregation with and without an external magnetic field. The various types of interparticle forces that are important in the dynamics of the aggregation process, such as dipole-dipole interactions, van der Waals forces, electrostatic forces and Brownian effects, are taken into account through the incorporation of the respective force models into the classical DEM model. The effects of overall solid fraction and the presence or absence of an external magnetic field on the propensity of such magnetic nanoparticles to aggregate and the microstructure of the resulting clusters or chain-like assemblies formed are investigated computationally.

2. Computational model

2.1 Discrete element method

The molecular dynamics approach to modeling of particulate systems, otherwise known as the Discrete Element Method (DEM), has been applied extensively for studies of flow behaviors in various types of granular and multiphase systems (Lim et al., 2006a, 2006b; Lim and Wang, 2006; Lim et al., 2007; Lim, 2007, 2008, 2009, 2010a, 2010b; Lim et al., 2011). For a comprehensive review, the interested reader is referred to a recent review article by Zhu et al. (2008). The methodology of DEM and its corresponding governing equations have also been presented numerous times in the research literature and only a brief description will be presented here for sake of completeness.

The translational and rotational motions of individual solid particles are governed by Newton's laws of motion:

$$m_i \frac{dv_i}{dt} = \sum_{j=1}^{N} \left(f_{c,ij} + f_{d,ij} \right) + f_{f,i} + f_{dd,ij} + f_{vdw,ij} + f_{e,ij} + f_{B,i} + f_{\mathrm{lub},ij} \tag{1}$$

$$I_i \frac{d\omega_i}{dt} = \sum_{j=1}^{N} T_{ij} \tag{2}$$

where m_i and v_i are the mass and velocity of the i^{th} particle respectively, N is the number of particles in contact with the i^{th} particle, $f_{c,ij}$ and $f_{d,ij}$ are the contact and viscous contact damping forces respectively, $f_{f,i}$ is the fluid drag force that is governed by Stokes' Law, $f_{dd,ij}$ is the dipole-dipole interaction between particles i and j in the presence of an applied magnetic field, $f_{vdw,ij}$ and $f_{e,ij}$ are the van der Waals interaction and electrostatic repulsion between particles i and j respectively, $f_{B,i}$ is the random force arising due to Brownian effects, $f_{lub,ij}$ is the lubrication force due to hydrodynamic effects, I_i is the moment of inertia of the i^{th} particle, ω_i is its angular velocity and T_{ij} is the torque arising from contact forces which causes the particle to rotate. The effect of gravity is neglected in the present study.

Contact and damping forces have to be calculated using force-displacement models that relate such forces to the relative positions, velocities and angular velocities of the colliding particles. A linear spring-and-dashpot model is implemented for the calculation of these collision forces. With such a closure, interparticle collisions are modeled as compressions of a perfectly elastic spring while the inelasticities associated with such collisions are modeled by the damping of energy in the dashpot component of the model. The normal ($f_{cn,ij}$, $f_{dn,ij}$) and tangential ($f_{ct,ij}$, $f_{dt,ij}$) components of the contact and damping forces are calculated according to the following equations:

$$f_{cn,ij} = -\left(\kappa_{n,i} \delta_{n,ij} \right) n_i \tag{3}$$

$$f_{ct,ij} = -\left(\kappa_{t,i} \delta_{t,ij} \right) t_i \tag{4}$$

$$f_{dn,ij} = -\eta_{n,i} \left(v_r \cdot n_i \right) n_i \tag{5}$$

$$f_{dt,ij} = -\eta_{t,i}\left\{\left(v_r \cdot t_i\right)t_i + \left(\omega_i \times R_i - \omega_j \times R_j\right)\right\} \tag{6}$$

where $\kappa_{n,i}$, $\delta_{n,ij}$, n_i, $\eta_{n,i}$ and $\kappa_{t,i}$, $\delta_{t,ij}$, t_i, $\eta_{t,i}$ are the spring constants, displacements between particles, unit vectors and viscous contact damping coefficients in the normal and tangential directions respectively, v_r is the relative velocity between particles and R_i and R_j are the radii of particles i and j respectively. If $\left|f_{ct,ij}\right| > \left|f_{cn,ij}\right|\tan\phi$, then 'slippage' between two contacting surfaces is simulated based on Coulomb-type friction law, i.e. $\left|f_{ct,ij}\right| = \left|f_{cn,ij}\right|\tan\phi$, where tan ϕ is analogous to the coefficient of friction.

2.2 Long range interactions

In the presence of an externally applied magnetic field, paramagnetic nanoparticles can be considered as magnetic single-domains with a permanent magnetic moment, μ_i proportional to their volume, $\mu_i = \frac{\pi d_i^3}{6} M_i$, where M_i is the intensity of magnetization. By the superparamagnetic magnetization law for a monodisperse, colloidal ferrofluid (Rosensweig, 1985),

$$\frac{M_i}{\phi_s M_d} = \coth\alpha_i - \frac{1}{\alpha_i} \tag{7}$$

where $\alpha_i = \frac{\pi}{6}\frac{\mu_o M_d H d_i^3}{kT}$, μ_o is the magnetic permeability of free space, M_d is the saturation magnetization of the bulk magnetic solid, H is the magnetic field strength, k is the Boltzmann's constant, T is thermodynamic temperature and ϕ_s is the volume fraction of solid present. The anisotropic dipole-dipole interaction energy $E_{dd,ij}$ is then given by (Rosensweig, 1985)

$$E_{dd,ij} = \frac{1}{4\pi\mu_o}\left[\frac{\mu_i \cdot \mu_j}{r_{ij}^3} - \frac{3}{r_{ij}^5}\left(\mu_i \cdot r_{ij}\right)\left(\mu_j \cdot r_{ij}\right)\right] \tag{8}$$

where μ_i and μ_j are the magnetic moments of particles i and j respectively and r_{ij} is the displacement vector between the two particles. The dipole-dipole force of interaction acting on particle i is then derived from $f_{dd,ij} = -\nabla E_{dd,ij}$.

The van der Waals forces of interaction and electrostatic repulsion between particles are calculated as follows (Russel et al., 1989):

$$f_{vdw,ij} = \frac{H_a}{6}\frac{d_i^6}{\left(h_{ij}^2 + 2d_i h_{ij}\right)^2\left(h_{ij} + d_i\right)^3} n_i \tag{9}$$

where H_a is the Hamaker constant and h_{ij} is the surface-to-surface separation distance along the line of centers of particles i and j. When the actual surface-to-surface separation distance between two particles is less than 1 nm, h_{ij} is fixed at 1 nm to avoid the singularity in the above equation.

The electrostatic repulsion between particles due to the so called double layer forces is described by the DLVO theory (Russel et al., 1989):

$$f_{e,ij} = 2\pi\varepsilon\varepsilon_o\left(\frac{kT}{ze}\right)^2 \kappa R_i q^2 \frac{\exp\left(-\kappa h_{ij}\right)}{1-\exp\left(-\kappa h_{ij}\right)} \tag{10}$$

where ε is relative permittivity, ε_o is the absolute permittivity of free space, z is the valency of ions, q is the surface charge, e is the fundamental electronic charge, κ^{-1} is the Debye decay length given by $\kappa^{-1} = \left(\frac{\varepsilon\varepsilon_o kT}{2e^2 z^2 n_b}\right)^{1/2}$, n_b is the concentration of ions.

For the size of nanoparticles simulated, it is also pertinent to consider the random forces arising due to Brownian effects. The algorithm for simulating Brownian forces is similar to that for generating a Gaussian white noise process (Russel et al., 1989):

$$f_{B,i} = \sqrt{12\pi\mu_f\left(\frac{d_i}{2}\right)kT\Delta t}\ n_i' \tag{11}$$

where Δt is the time step used in the simulation and n_i' is a unit vector with a random direction. It is well-established that Brownian effects become less significant at small separation distances between particles due to the presence of hydrodynamic lubrication effects. As such, Brownian forces were set to zero for surface-to-surface distances less than 1 nm in all simulations.

2.3 Hydrodynamic interactions

Hydrodynamic interactions due to lubrication effects become important at small surface-to-surface separation distances between particles. The lubrication force between two spheres is described by the lubrication theory and may be calculated as follows (Russel et al., 1989):

$$f_{\text{lub},ij} = \frac{6\pi\mu\left(v_r \cdot n_i\right)}{h_{ij}}\frac{d_i^2}{16}n_i \tag{12}$$

Here, as with the calculation of van der Waals forces described earlier, when the surface-to-surface separation distance between two particles is less than 1 nm, h_{ij} is fixed at 1 nm to avoid the singularity in the above equation.

3. Simulation conditions

The simulation conditions applied were based as much as possible on the materials and methods used for experimental studies reported in the literature so that a meaningful comparison between the simulations and experiments can be made. Spherical nanoparticles of diameter 70 nm and density 1000 kg m^{-3} were simulated within a pseudo-three-dimensional computational domain. The dimensions of the computational domain were 5 μm × 5 μm with thickness in the spanwise direction equivalent to one particle diameter. The

numbers of nanoparticles simulated were 485, 975, 1460 and 1950 which correspond to solid volume fractions of 0.05, 0.10, 0.15 and 0.20 respectively. Here, solid volume fraction is defined to be the ratio of the total volume of all nanoparticles present to the volume of the pseudo-three-dimensional domain. To ensure numerical stability and accuracy, a relatively small time step of 10 ps was applied for all simulations carried out in this study. Table 1 summarizes the values of pertinent material properties and system parameters applied in the simulations. At the start of each simulation, the positions of all nanoparticles were assigned randomly within the computational domain such that no overlap between any two nanoparticles occurred. Periodic boundary conditions were applied on all four sides of the computational domain so as to eliminate any possible effects that may arise due to the presence of boundaries. The application of such boundary conditions also allowed the possibility of simulating a large system using a significantly smaller computational domain which leads to more efficient utilization of computing resources.

Shape of particles	Spherical
Number of particles, N	485, 975, 1460, 1950
Solid volume fraction	0.05, 0.10, 0.15, 0.20
Particle diameter, d	70 nm
Particle density, ρ_p	1000 kg m^{-3}
Spring constant in force model, κ	1.0×10^{-3} N m^{-1}
Viscous contact damping coefficient, η	1.0×10^{-12}
Coefficient of restitution	0.99
Coefficient of friction	0.5
Saturation magnetization, M_d	1.0×10^{5} A m^{-1}
Hamaker constant, H_a	1.0×10^{-19} J
Surface charge, q	1.6×10^{-15} C
Ion concentration, n_b	1.0 M
Temperature, T	298 K
Domain size	5 μm × 5 μm × 70 nm
Simulation time step, Δt	10 ps

Table 1. Material properties and system parameters for DEM simulations

4. Results and discussion

Fig. 1 shows the aggregation patterns of magnetic nanoparticles formed in the absence of an external magnetic field obtained from computer simulations with the modified DEM methodology. It may be seen that small isolated aggregates of nanoparticles are observed at low solid volume fractions while at high solid volume fractions, an extended network of nanoparticles usually referred to as a percolated network is observed to form spontaneously. The former is typically associated with gelation experiments carried out at insufficient concentrations of nanoparticles resulting in simple destabilisation of the suspension and formation of a collapsed structure.

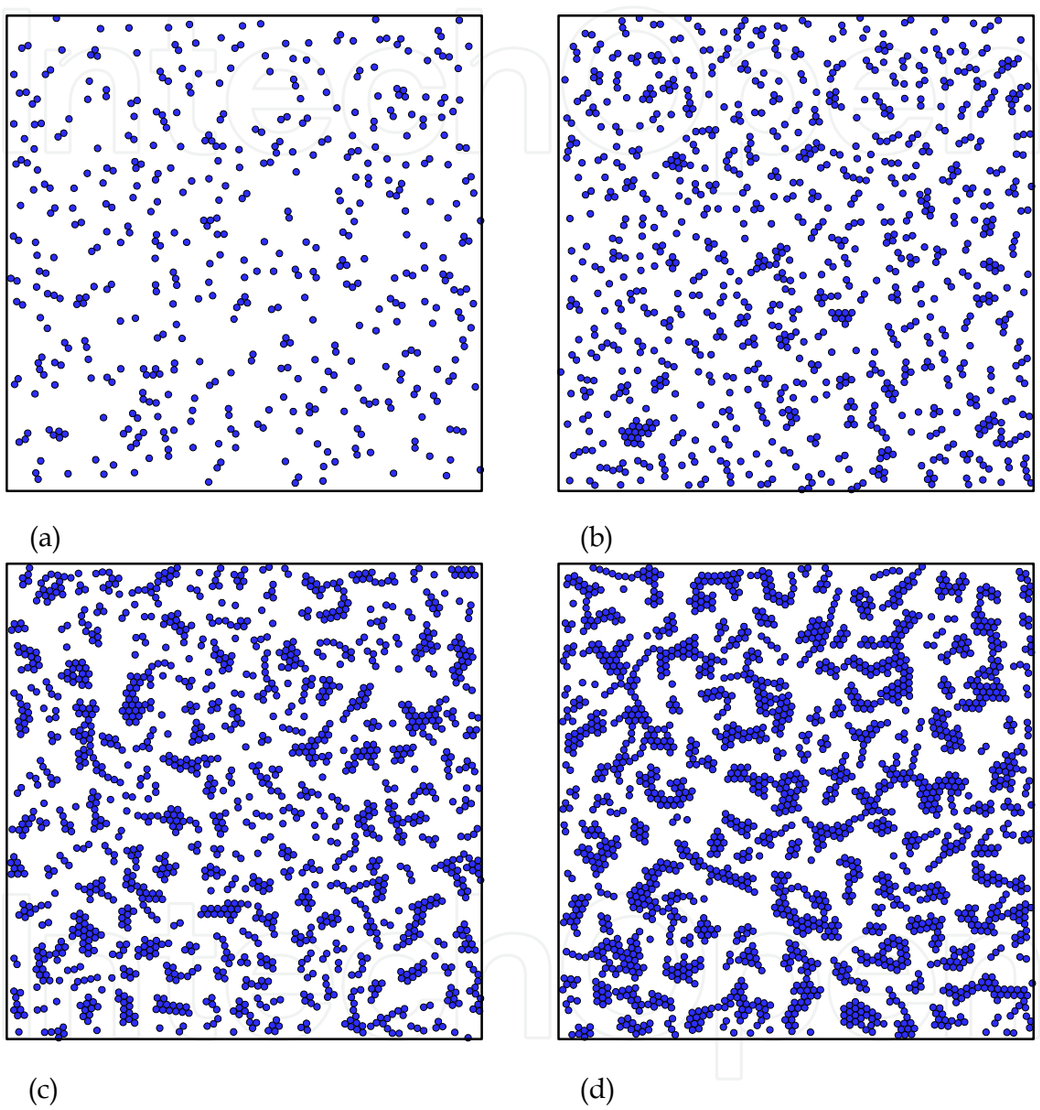

Fig. 1. Aggregation patterns of magnetic nanoparticles in the absence of an external magnetic field at 10^{-3} s physical time obtained from the modified DEM simulations. The solid volume fractions applied were (a) 0.05, (b) 0.10, (c) 0.15 and (d) 0.20.

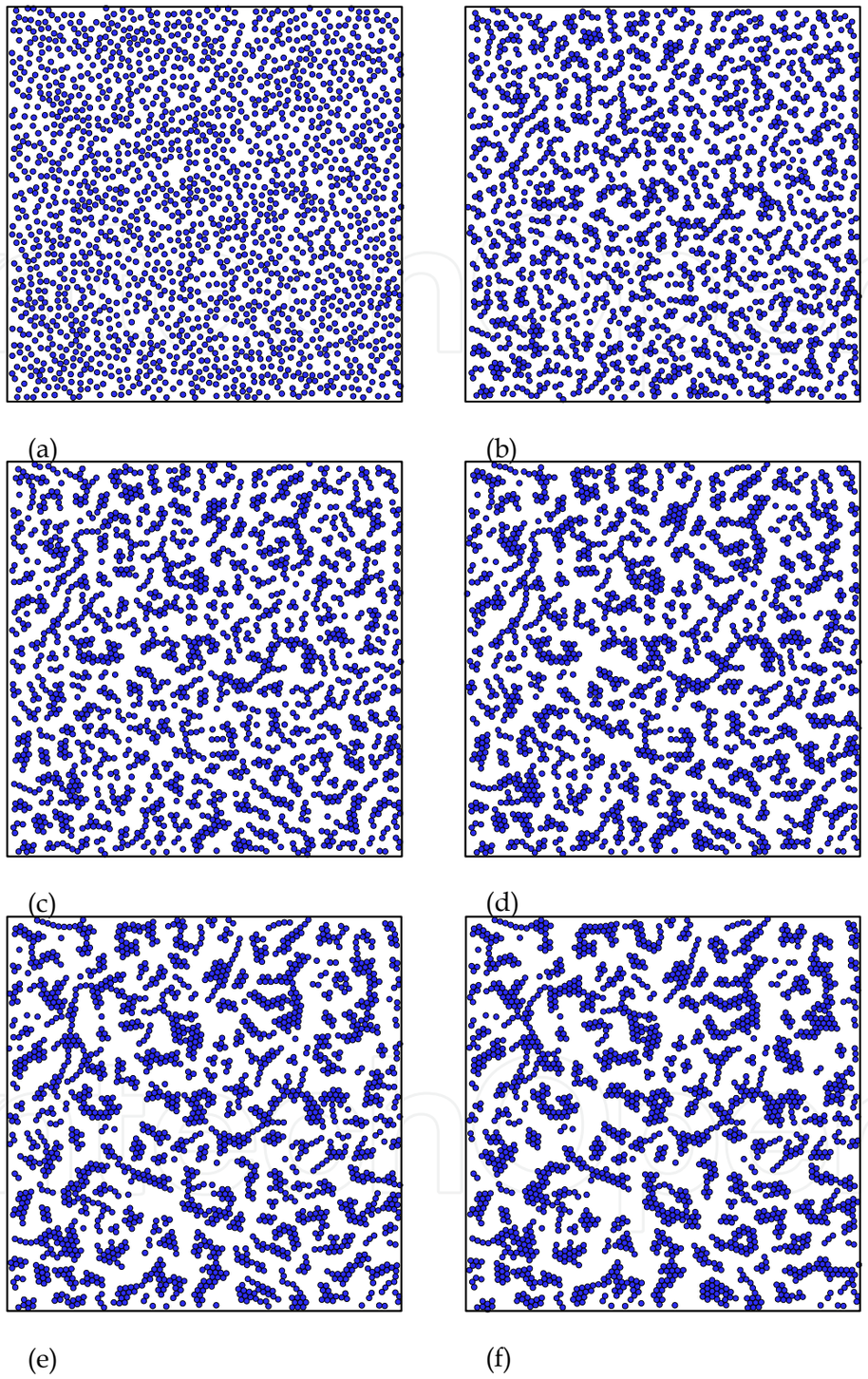

Fig. 2. Aggregation process of magnetic nanoparticles of solid volume fraction 0.20 in the absence of an external magnetic field. The states of aggregation correspond to (a) 0.0 s, (b) 2.0×10^{-4} s, (c) 4.0×10^{-4} s, (d) 6.0×10^{-4} s, (e) 8.0×10^{-4} s and (f) 10^{-3} s.

To observe gelation of nanoparticle suspensions, the present simulations have shown that solid concentrations must be sufficiently high and beyond the percolation threshold in order for a stable network structure to form. Although the simulations presented here are computationally expensive and so have been carried out at smaller length and time scales than those associated with experiments, it may be seen that the main qualitative features of the type of gel networks formed in the absence of an external magnetic field have been reproduced computationally. In particular, Fig. 2 shows that the gelation process takes place with the initial formation of small random aggregates throughout the domain which then join to form a fairly open network with no specific orientation of the various branches.

The intermediate states of the gel during its formation process that are unobservable experimentally with present day technology are readily available from DEM simulations. With the advent of computing power, this computational technique is expected to become more important in this research field as such information will be necessary for more fundamental and mechanistic understanding of nanoparticle gelation processes. Fig. 3 shows that in the presence of an external magnetic field, the aggregates of nanoparticles are aligned along the direction of the magnetic field due to the anisotropic nature of the magnetic forces exerted on each nanoparticle and aggregate. At low solid volume fractions, individual elongated strands of aggregates are formed while at high solid volume fractions, such aggregates are capable of joining together due to smaller distances between aggregates. In comparison with the previous case where an external magnetic field was absent, the branches of the network that is beginning to form here are composed of more particles and are thus longer. This can be understood from inspection of the intermediate states of aggregation obtained from the simulations.

Fig. 4 shows that the aggregation process in the presence of an external magnetic field starts, as in the previous case, with the formation of random aggregates throughout the domain. However, due to the anisotropic magnetic forces, aggregates formed are rotated to align along the direction of the magnetic field. Elongation of aggregates occurs as the growth of these aggregates also occurs along the direction of the magnetic field imposed. The final network structure consisting of long, parallel chains of nanoparticles is also in good agreement with structures of gels obtained experimentally with an applied magnetic field.

Fig. 5 shows quantitatively the time evolution of the average sizes of clusters formed by the magnetic nanoparticles both in the absence and presence of an external magnetic field. Here, average cluster size is defined as the average number of nanoparticles forming a cluster or aggregate. It may be observed that average cluster sizes increase with increasing total number of nanoparticles present within the domain or, equivalently, the overall solid volume fraction. Interestingly, the average size of clusters formed at each solid volume fraction evolves in a similar fashion with respect to time regardless of the presence or absence of an external magnetic field. This is despite the fact that the morphologies of the clusters or aggregates formed are significantly different as seen earlier. At the end of 1 ms, the average cluster sizes for N = 485 and N = 975 both in the absence and presence of an external magnetic field have reached more or less steady values. In contrast, the clusters formed for N = 1460 and N = 1950 are still growing in size, indicating that the percolation process is not completed yet at the end of 1 ms.

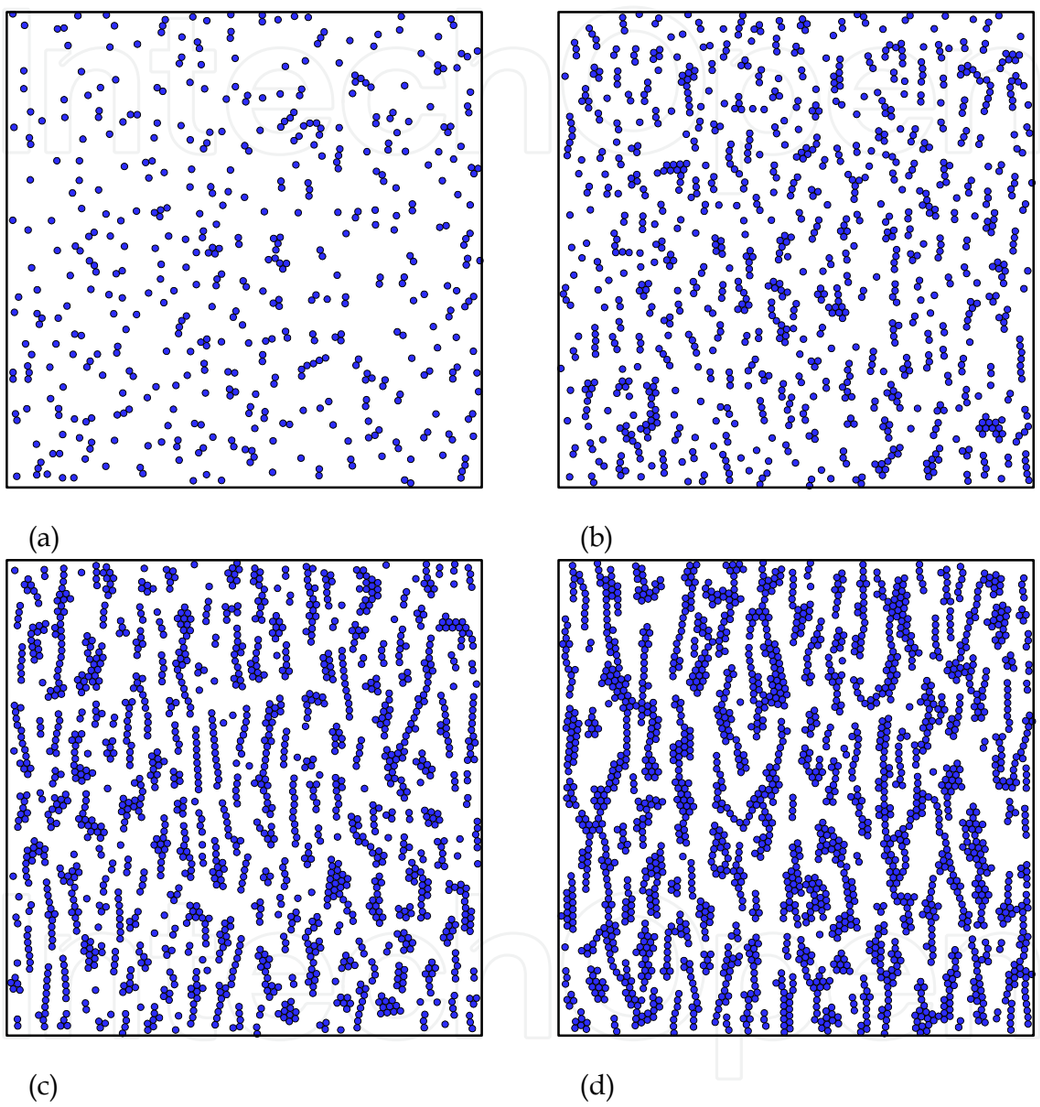

Fig. 3. Aggregation patterns of magnetic nanoparticles in the presence of an external magnetic field at 10^{-3} s physical time obtained from the modified DEM simulations. The orientation of the simulated magnetic field was in the vertical direction. The solid volume fractions applied were (a) 0.05, (b) 0.10, (c) 0.15 and (d) 0.20.

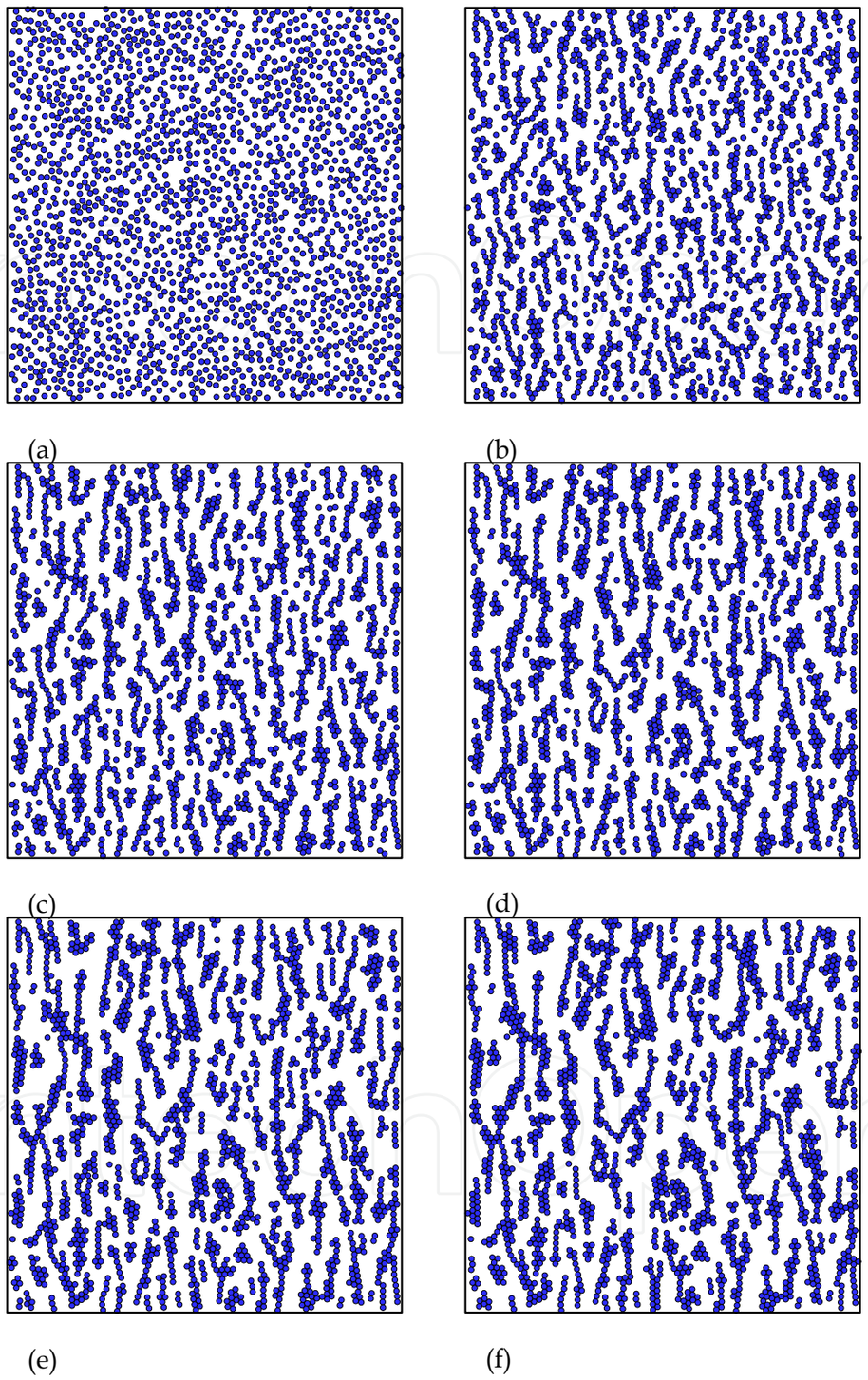

Fig. 4. Aggregation process of magnetic nanoparticles of solid volume fraction 0.20 in the presence of an external magnetic field. The states of aggregation correspond to (a) 0.0 s, (b) 2.0×10^{-4} s, (c) 4.0×10^{-4} s, (d) 6.0×10^{-4} s, (e) 8.0×10^{-4} s and (f) 10^{-3} s.

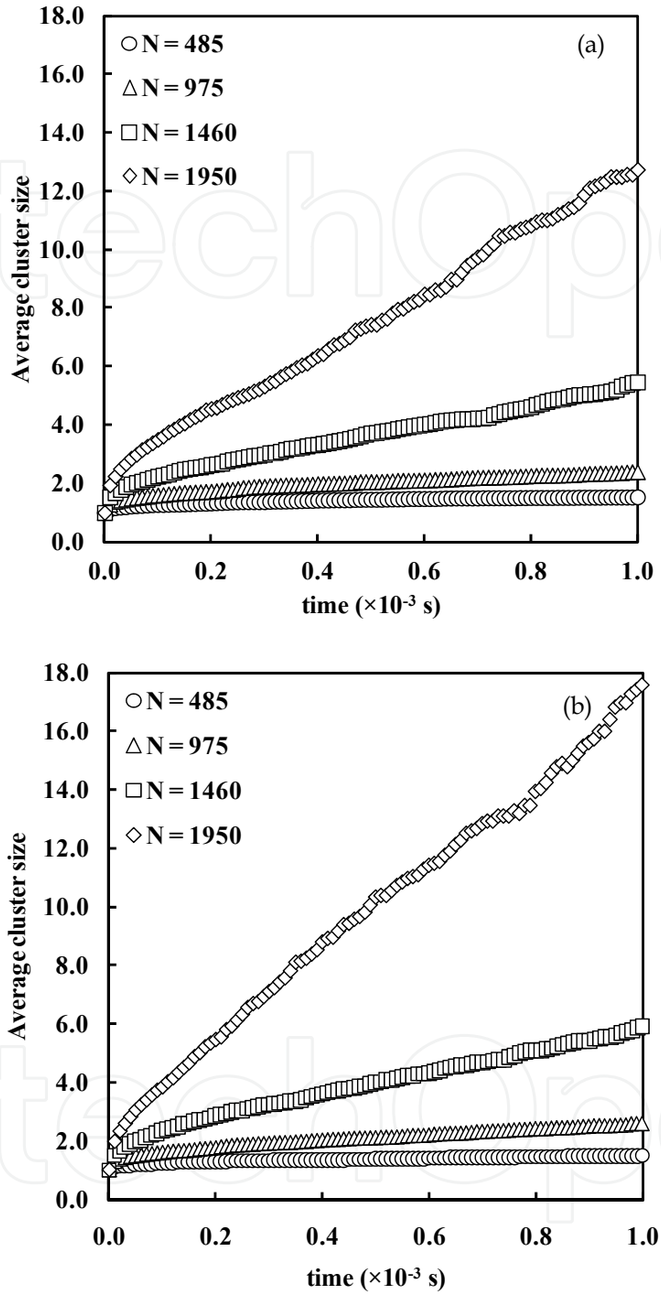

Fig. 5. Time evolution of average size of clusters formed by magnetic nanoparticles (a) in the absence of an external magnetic field and (b) in the presence of an external magnetic field.

5. Conclusions

The process of gelation with and without the application of an external magnetic field giving rise to the different internal pore structures could be understood mechanistically by results of

the simulations performed using a modified Discrete Element Method. Gelation occurred by the formation of random aggregates of nanoparticles within the domain which then joined with one another to form a network. However, in the presence of anisotropic magnetic forces, these aggregates were rotated to align along the direction of the magnetic field. Elongation of aggregates occurred and the final network formed consisted largely of such elongated branches of magnetic nanoparticles arranged more or less parallel to one another.

6. Acknowledgment

This study has been supported by the National University of Singapore under Grant Number R-279-000-275-112.

7. References

Brunet, E.; Degre, G.; Okkels, F.; Tabeling, P. (2005). Aggregation of Paramagnetic Particles in the Presence of a Hydrodynamic Shear. *J. Colloid Interface Sci.*, Vol. 282, pp. 58–68

Climent, E.; Maxey, M. R.; Karniadakis, G. E. (2004). Dynamics of Self-Assembled Chaining in Magnetorheological Fluids. *Langmuir*, Vol. 20, pp. 507–513

Davis, S. W.; McCausland, W.; McGahagan, H. C.; Tanaka, C. T.; Widom, M. (1999). Cluster-based Monte Carlo Simulation of Ferrofluids. *Phys. Rev. E*, Vol. 59, pp. 2424–2428

Dominguez-Garcia, P.; Melle, S.; Pastor, J. M.; Rubio, M. A. (2007). Scaling in the Aggregation Dynamics of a Magnetorheological Fluid. *Phys. Rev. E*, Vol. 76, pp. 051403

Duncan, P. D.; Camp, P. J. (2006). Aggregation Kinetics and the Nature of Phase Separation in Two-Dimensional Dipolar Fluids. *Phys. Rev. Lett.*, Vol. 97, pp. 107202

Furlani, E. P. (2006). Analysis of Particle Transport in a Magnetophoretic Microsystem. *J. Appl. Phys.*, Vol. 99, pp. 024912

Furlani, E. P.; Ng, K. C. (2008). Nanoscale Magnetic Biotransport with Application to Magnetofection. *Phys. Rev. E*, Vol. 77, pp. 061914

Huang, J. P.; Wang, Z. W.; Holm, C. (2005). Computer Simulations of the Structure of Colloidal Ferrofluids. *Phys. Rev. E*, Vol. 71, pp. 061203

Kantorovich, S.; Cerda, J. J.; Holm, C. (2008). Microstructure Analysis of Monodisperse Ferrofluid Monolayers: Theory and Simulation. *Phys. Chem. Chem. Phys.*, Vol. 10, pp. 1883–1895

Lattuada, M.; Alan Hatton, T. (2007). Preparation and Controlled Self-Assembly of Janus Magnetic Nanoparticles. *J. Am. Chem. Soc.*, Vol. 129, pp. 12878–12889

Lattuada, M.; Wu, H.; Sandkuhler, P.; Sefcik, J.; Morbidelli, M. (2004a). Modelling of Aggregation Kinetics of Colloidal Systems and its Validation by Light Scattering Measurements. *Chem. Eng. Sci.*, Vol. 59, pp. 1783–1798

Lattuada, M.; Wu, H.; Morbidelli, M. (2004b). Experimental Investigation of Colloidal Gel Structures. *Langmuir*, Vol. 20, pp. 4355–4362

Lim, E. W. C.; Wang, C. H., Yu, A. B. (2006a). Discrete Element Simulation for Pneumatic Conveying of Granular Material. *AIChE J.*, Vol. 52, pp. 496–509

Lim, E. W. C.; Zhang, Y.; Wang, C. H. (2006b). Effects of an Electrostatic Field in Pneumatic Conveying of Granular Materials through Inclined and Vertical Pipes. *Chem. Eng. Sci.*, Vol. 61, pp. 7889–7908

Lim, E. W. C.; Wang, C. H. (2006). Diffusion Modeling of Bulk Granular Attrition. *Ind. Eng. Chem. Res.*, Vol. 45, pp. 2077–2083

Lim, E. W. C.; Wong, Y. S.; Wang, C. H. (2007). Particle Image Velocimetry Experiment and Discrete-Element Simulation of Voidage Wave Instability in a Vibrated Liquid-Fluidized Bed. *Ind. Eng. Chem. Res.*, Vol. 46, pp. 1375–1389

Lim, E. W. C. (2007). Voidage Waves in Hydraulic Conveying through Narrow Pipes. *Chem. Eng. Sci.*, Vol. 62, pp. 4529–4543

Lim, E. W. C. (2008). Master Curve for the Discrete-Element Method. *Ind. Eng. Chem. Res.*, Vol. 47, pp. 481–485

Lim, E. W. C. (2009). Vibrated Granular Bed on a Bumpy Surface. *Phys. Rev. E*, Vol. 79, pp. 041302

Lim, E. W. C. (2010a). Density Segregation in Vibrated Granular Beds with Bumpy Surfaces. *AIChE J.*, Vol. 56, pp. 2588–2597

Lim, E. W. C. (2010b). Granular Leidenfrost Effect in Vibrated Beds with Bumpy Surfaces. *Eur. Phys. J. E*, Vol. 32, pp. 365–375

Lim, E. W. C.; Yao, J.; Zhao, Y. (2011). Pneumatic Transport of Granular Materials with Electrostatic Effects. *AIChE J.*, Article in Press, DOI 10.1002/aic.12638

Martinez-Pedrero, F.; El-Harrak, A.; Fernandez-Toledano, J. C.; Tirado-Miranda, M.; Baudry, J.; Schmitt, A.; Bibette, J.; Callejas-Fernandez, J. (2008). Kinetic Study of Coupled Field-Induced Aggregation and Sedimenation Processes Arising in Magnetic Fluids. *Phys. Rev. E*, Vol. 78, pp. 011403

Meriguet, G.; Jardat, M.; Turq, P. (2004). Structural Properties of Charge-Stabilized Ferrofluids under a Magnetic Field: A Brownian Dynamics Study. *J. Chem. Phys.*, Vol. 121, pp. 6078–6085

Meriguet, G.; Jardat, M.; Turq, P. (2005). Brownian Dynamics Investigation of Magnetization and Birefringence Relaxations in Ferrofluids. *J. Chem. Phys.*, Vol. 123, pp. 144915

Miyazima, S.; Meakin, P.; Family, F. (1987). Aggregation of Oriented Anisotropic Particles. *Phys. Rev. A*, Vol. 36, pp. 1421–1427

Nandy, K.; Chaudhuri, S.; Ganguly, R.; Puri, I. K. (2008). Analytical Model for the Magnetophoretic Capture of Magnetic Microspheres in Microfluidic Devices. *J. Magn. Magn. Mater.*, Vol. 320, pp. 1398–1405

Pamme, N. (2006). Magnetism and Microfluidics. *Lab Chip*, Vol. 6, pp. 24–38

Promislow, J. H. E.; Gast, A. P.; Fermigier, M. (1995). Aggregation Kinetics of Paramagnetic Colloidal Particles. *J. Chem. Phys.*, Vol. 102, pp. 5492–5498

Richardi, J.; Pileni, M. P.; Weis, J.-J. (2008). Self-organization of Magnetic Nanoparticles: A Monte Carlo Study. *Phys. Rev. E*, Vol. 77, pp. 061510

Rosensweig, R. E. (1985). *Ferrohydrodynamics*, Cambridge University Press

Russel, W. B.; Saville, D. A.; Schowalter, W. R. (1989). *Colloidal Dispersions*, Cambridge University Press

Schaller, V.; Kraling, U.; Rusu, C.; Petersson, K.; Wipenmyr, J.; Krozer, A.; Wahnstrom, G.; Sanz-Velasco, A.; Enoksson, P.; Johansson, C. (2008). Motion of Nanometer Sized Magnetic Particles in a Magnetic Field Gradient. *J. Appl. Phys.*, Vol. 104, pp. 093918

Sinha, A.; Ganguly, R.; De, A. K.; Puri, I. K. (2007). Single Magnetic Particle Dynamics in a Microchannel. *Phys. Fluids*, Vol. 19, pp. 117102

Tsouris, C.; Scott, T. C. (1995). Flocculation of Paramagnetic Particles in a Magnetic Field. *J. Colloid Interface Sci.*, Vol. 171, pp. 319–330

Xuan, Y.; Ye, M.; Li, Q. (2005). Mesoscale Simulation of Ferrofluid Structure. *Int. J. Heat Mass Trans.*, Vol. 48, pp. 2443–2451

Yamada, Y.; Enomoto, Y. (2008). Effects of Oscillatory Shear Flow on Chain-like Cluster Dynamics in Ferrofluids without Magnetic Fields. *Physica A*, Vol. 387, pp. 1–11

Zhu, H. P.; Zhou, Z. Y.; Yang, R. Y.; Yu, A. B. (2008). Discrete Particle Simulation of Particulate Systems: A Review of Major Applications and Findings. *Chem. Eng. Sci.*, Vol. 63, pp. 5728–5770

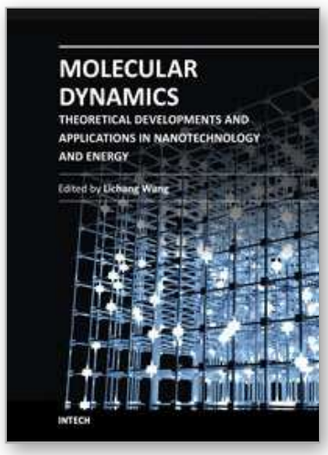

Molecular Dynamics - Theoretical Developments and Applications in Nanotechnology and Energy

Edited by Prof. Lichang Wang

ISBN 978-953-51-0443-8
Hard cover, 424 pages
Publisher InTech
Published online 05, April, 2012
Published in print edition April, 2012

Molecular Dynamics is a two-volume compendium of the ever-growing applications of molecular dynamics simulations to solve a wider range of scientific and engineering challenges. The contents illustrate the rapid progress on molecular dynamics simulations in many fields of science and technology, such as nanotechnology, energy research, and biology, due to the advances of new dynamics theories and the extraordinary power of today's computers. This first book begins with a general description of underlying theories of molecular dynamics simulations and provides extensive coverage of molecular dynamics simulations in nanotechnology and energy. Coverage of this book includes: Recent advances of molecular dynamics theory Formation and evolution of nanoparticles of up to 106 atoms Diffusion and dissociation of gas and liquid molecules on silicon, metal, or metal organic frameworks Conductivity of ionic species in solid oxides Ion solvation in liquid mixtures Nuclear structures

INTECH
open science | open minds

InTech Europe
University Campus STeP Ri
Slavka Krautzeka 83/A
51000 Rijeka, Croatia
Phone: +385 (51) 770 447
Fax: +385 (51) 686 166
www.intechopen.com

InTech China
Unit 405, Office Block, Hotel Equatorial Shanghai
No.65, Yan An Road (West), Shanghai, 200040, China
中国上海市延安西路65号上海国际贵都大饭店办公楼405单元
Phone: +86-21-62489820
Fax: +86-21-62489821

IntechOpen